Study of chiral recognition of model peptides and odorants: Carvone and camphor

N. Nandi

Chemistry Department, Birla Institute of Technology and Science, Pilani 333 031, India

An atomistic calculation of the interaction between peptide motifs and enantiomeric odorant molecules (carvone and camphor) is performed. The peptide motifs are mimics of segments of the helical receptor structure. The model shows that the enantiomers of carvone have distinctly different interaction profile with all peptides considered, but the enantiomers of camphor do not exhibit any significant enantiodifference. This parallels the experimental fact that the enantiomers of carvone have different smells, while those of camphor cannot be discriminated by olfaction. This is expected to be a pilot study in further atomistic calculations to understand molecular recognition in olfaction process.

CHIRAL discrimination has tremendous importance in biological and biomimetic systems[1,2]. Nature has strong chiral preference at all levels of structural hierarchy, from micro- to meso- to macroscopic organizations. Most common examples are proteins and their constituent amino acids, nucleic acids and their constituent sugars as well as membranes and their constituent lipids and membrane proteins. While the structural difference between the enantiomers of the basic building blocks (like amino acid, sugar, lipid) are only subtle; the higher level structures (such as protein, nucleic acid and membrane) are active with only one enantiomeric form of the basic subunit. Why nature prefers only one enantiomer of its building blocks remained a puzzle. Understanding the reason for chiral preference shown by nature has also tremendous practical applications. Single enantiomeric drugs constitute more than 30% of the total therapeutic drugs used in recent years. However, a molecular level understanding of the chiral discrimination of biological molecules is still in its infancy.

Like other chiral recognition processes, discrimination of enantiomeric odorant molecules by olfaction is a complex process and is not understood in molecular detail. While the simpler biomimetic systems exhibit either heterochiral or homochiral preference (with varying degree) in all known cases of biomimetic recognition, olfactory recognition is dependent on chirality for specific cases. For example, while α-pinene, carvone and limonene can be discriminated based on their odour quality, no significant olfactory discrimination is reported[3–8] for the enantiomers of camphor, menthol, rose oxide, α-terpineol, β-citronellol and 2-butanol. It is observed that the presence or absence of a certain functional group at the chiral carbon atom or membership of a certain chemical class is not a sufficient condition that the corresponding enantiomers will be discriminable by olfaction. It is known that enantiomeric odorants give rise to olfactory discrimination of various degrees[6,8]. The two existing major theories of olfactory recognition, namely the stereochemical theory and the vibrational theory, fail to explain the odour difference of isomeric compounds[9–11].

It was expected that the G-protein coupled transmembrane (TM) olfactory receptor (OR) helices being chiral at all levels of structure (primary to quaternary), the molecular chiral feature (or its absence) of OR and odorant may play a role in odorant recognition. Recent studies have shown that the chirality present in a peptide at its secondary level structure plays a significant role in orientation-dependent ligand–helical peptide recognition[12]. The study demonstrated that the two enantiomers of a ligand molecule have favourable interactions at different mutual helix–ligand orientations. Such differences in the helix orientations lead to different binding properties. It is thus worthwhile to investigate the role of the chiral structure of the odorant molecules and receptors as a primary event of olfaction cascade.

The binding processes between D- and L-enantiomers of a particular odorant (denoted by O_D and O_L, respectively) with an OR molecule (denoted by *Re*) can be represented as

$$O_D + Re \leftrightarrow O_D Re \tag{1}$$

$$O_L + Re \leftrightarrow O_L Re. \tag{2}$$

The respective equilibrium constants for the odorant–receptor interactions are given by

$$K_D = e^{-\Delta G_D / RT}, \quad K_L = e^{-\Delta G_L / RT}, \tag{3}$$

where ΔG_D and ΔG_L are the free energy changes corresponding to the binding processes described above and T is the temperature. One can relate the contribution of intermolecular interaction to free energy using standard statistical thermodynamic relations[13]. The Helmholtz free energy is re-

e-mail: nnandi@bits-pilani.ac.in

lated to the change in free energy in an isothermal isobaric (NPT) ensemble as

$$dG = dA + PdV + VdP, \quad (4)$$

Here A is the Helmholtz free energy, P is the pressure of the system and V is the volume. $A(V, T)$ is related to the partition function of the system, $Q(V, T)$ by the relation

$$A(V, T) = -k_B T \ln Q(V, T). \quad (5)$$

The potential energy contribution to the partition function is dependent on the configurational integral of the system, $Z_N(V, T)$ and the latter is related to the intermolecular potential $U_N(\vec{r}^N)$ by the relation

$$Z_N(V, T) = \int \exp[\beta U_N(\vec{r}^N)] d\vec{r}^N. \quad (6)$$

Suppose the odorant contains 1, 2, ... , i ,..., N atoms and receptor contains 1, 2, ... j, ..., N' atoms, then the total intermolecular potential, $U_N(\vec{r}^N)$ can be obtained by summing over the effective atom–atom pair potential, $U(\vec{r}_{ij}, \vec{\Omega}_{ij})$, where $\vec{r}_{ij}$, $\vec{\Omega}_{ij}$ are the mutual distance and orientation of the respective atom pairs of odorant and receptor. The effective atom–atom pair potential is dependent on the interatomic distance and orientation. Thus, binding of the two enantiomers can be discriminated if the intermolecular potential has different distance and orientation dependency in the two cases.

It is known that the odorant molecules are recognized by the guanine nucleotide binding protein (G-protein)-coupled olfactory receptors. Here, the odorant molecule is in contact with many transmembrane helices[14]. It is likely that there is a large family of receptor molecules (about 100–1000 members). These seven transmembrane domain proteins (TM7) are encoded by a large multigene family. The OR proteins have 300–350 amino acids. Obviously, numerous combinations of amino acids are possible, which can serve as binding sites. However, it is important to note that such an OR always works as a chiral entity for the odorant, irrespective of the amino acid sequence. Hence, it suffices for our purpose to study chiral discrimination by taking model peptide sequences, which can serve as helical chiral subunits of the receptor. If the interaction profiles of both enantiomers of the odorant with a given peptide turn out to be significantly different, then one can conclude a chiral discrimination. The nature of the $U_N(\vec{r}^N)$ profiles for equilibrium conditions described by eqs (1) and (2) (their distance and orientation dependence) for a particular peptide with each pair of enantiomers, will then reveal the discrimination.

The organization of the rest of the article is as follows. In the following section we present theoretical calculations. Next, the results are presented and discussed followed by concluding remarks.

Theoretical calculation

In the present article, we have investigated the interaction profile of enantiomeric pairs of carvone and camphor with four peptides composed of five residues. The chiral peptide structures are H–Leu–His–Thr–Pro–Met–OH (designated as Peptide 1), H–Met–Ala–Tyr–Asp–Arg–OH (designated as Peptide 2), H–Tyr–Val–Ala–Ile–Cys–OH (designated as Peptide 3) and H–Phe–Ser–Thr–Cys–Ser–OH (designated as Peptide 4) respectively. Although these sequences are observed in OR, they are used in the present work only as different helical chiral mimics of the receptor segments, which can be used to observe the discrimination of intermolecular interaction and no more. The energy minimized structures of the four peptides, carvone and camphor molecules are shown in Figure 1 *a–f* respectively.

The geometry of the molecule, net dipole moment as well as charges on the individual atoms are generated using MOPAC[15]. The theory used is at the semi-empirical PM3 level[16]. The charges are obtained using Mulliken population analysis (MPA) technique[16]. Variation of intermolecular potential is calculated as a function of mutual orientation and distance of the peptide and odorant (carvone and camphor). The geometry of the mutual arrangement considered is shown in Figure 1 *g*.

The intermolecular interaction energy between the enantiomer of the odorant and the peptide is given by a Lennard–Jones (LJ) potential (short-range repulsion and long-range attraction over all nonbonded pairs of atoms) supplemented by Coulombic interaction.

$$\sum_i^N \sum_j^{N'} (\vec{r}_{ij}, \vec{\Omega})_{D/L} / k_B T = \sum_i^N \sum_j^{N'} (4\varepsilon^{ij} / k_B T)[\boldsymbol{R}^{ij} / \sigma^{ij})^{-12} - (\boldsymbol{R}^{ij} / \sigma^{ij})^{-6}] + \sum_i^N \sum_j^{N'} (q_i q_j) / (4\pi\varepsilon_s \varepsilon_0 \boldsymbol{R}^{ij}). \quad (7)$$

Here $\boldsymbol{R}^{ij}$ is the orientation-dependent distance between the atoms i and j (of enantiomeric odorant and peptide respectively), σ^{ij} is the average LJ diameter of the corresponding atoms and the energy parameter ε^{ij} is given by the Berthelot rule, $\varepsilon^{ij} = (\varepsilon^i \varepsilon^j)^{1/2}$. Explicit expressions for the calculation of $\boldsymbol{R}^{ij}$ were developed earlier[1]. Charges on the ith and jth atom are designated as q_i and q_j, ε_s is the effective static dielectric constant of the medium and ε_0 is the vacuum permittivity. The LJ parameters are taken from OPLS potential parameter set[18]. Intermolecular interaction is calculated based on free energy functional given by eq. (7) with rigid geometry approximation for the pair of molecules. The optimized geometries obtained from semi-empirical PM3-based theory (as discussed previously) are used for both molecules. In the present work the dielectric constant of the medium is considered as 4 and 20, representative values of the limiting range of dielectric constant of the nonpolar membrane medium where the recognition

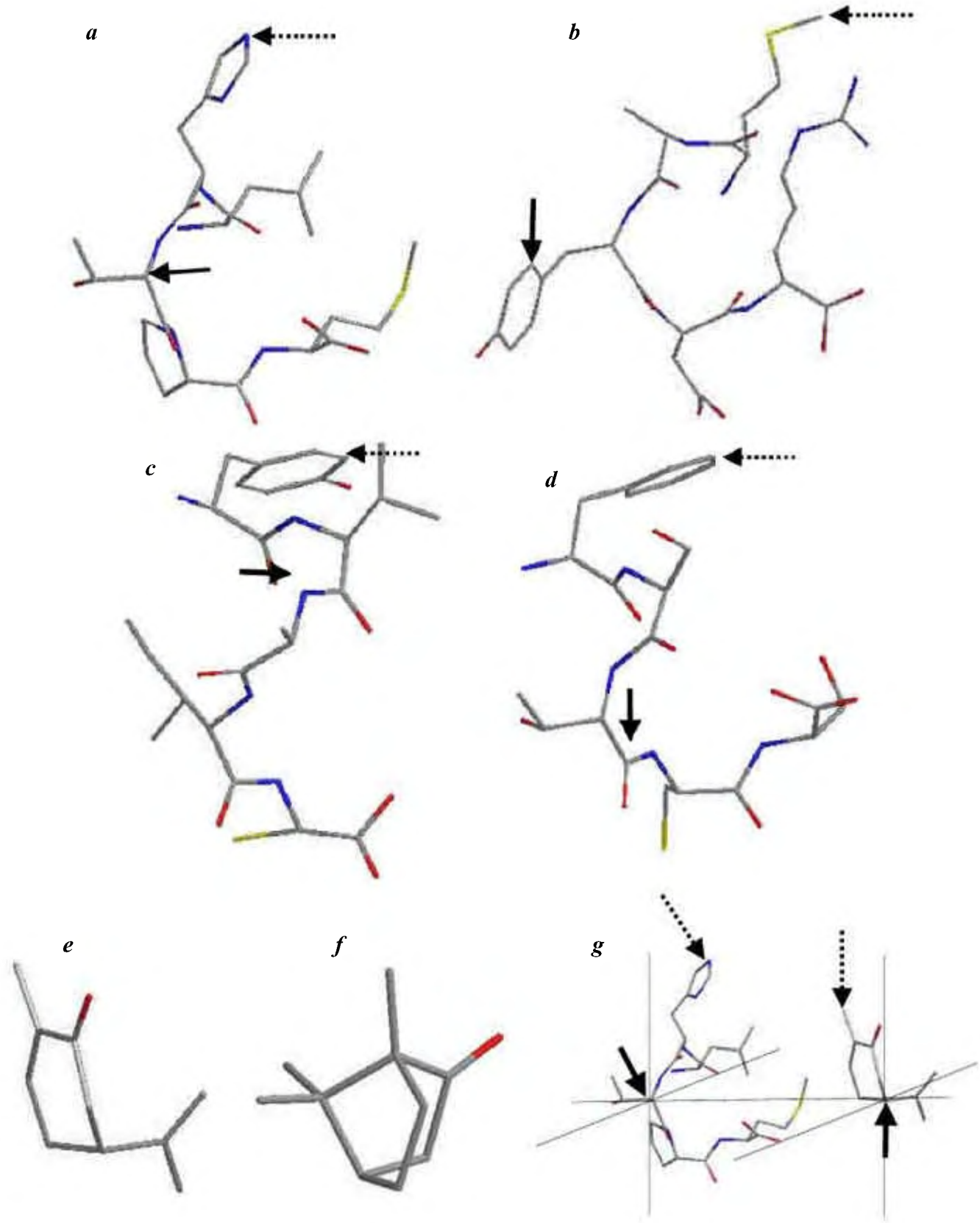

Figure 1 ***a–g.*** ***a–d***, Energy-minimized structures (as stick model) of Peptides 1–4. ***e***, ***f***, Energy-minimized structures of carvone and camphor. ***g***, Relative arrangement of peptide and odorant. Arbitrarily chosen centre of peptide and odorant is shown pointed by solid arrows and top end atoms of molecules (used to calculate azimuthal orientation) are shown by dotted arrows. While the position and orientation of a particular peptide are fixed at a given tilt and azimuthal orientation, the orientation of enantiomeric odorants is varied through 2π and simultaneously separated from the peptide to generate the potential profile. See text for detail.

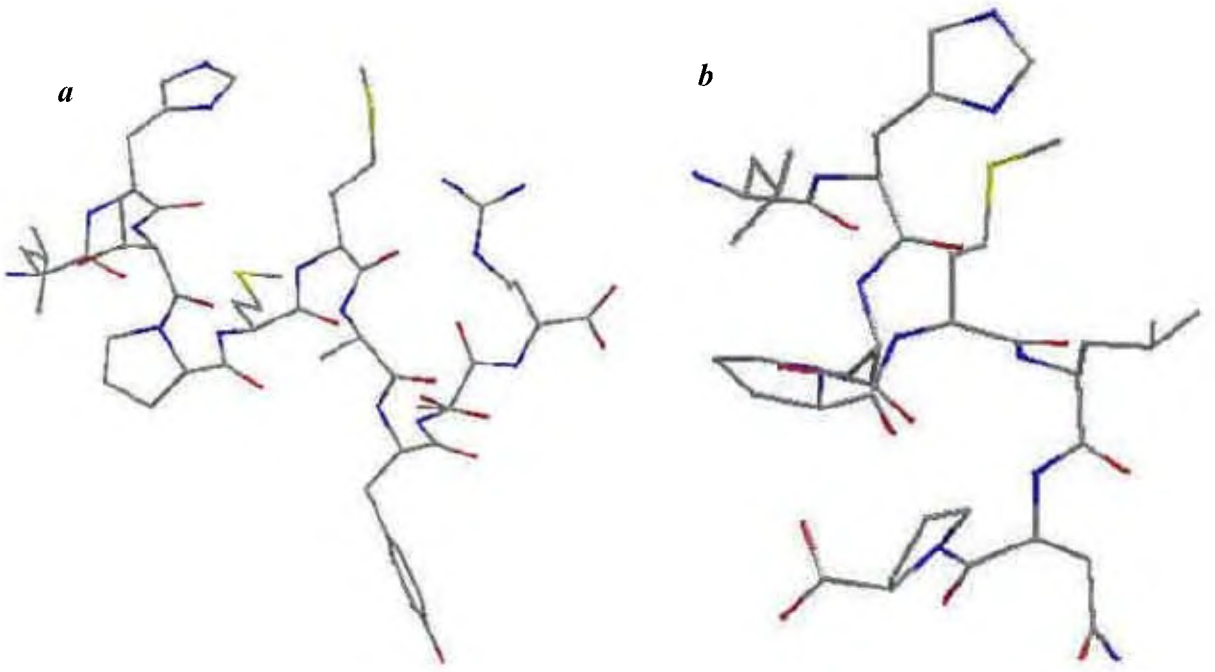

Figure 2. Energy-minimized structures of dipeptides formed by combination of Peptide 1 with Peptide 2 (designated as Peptide 12) and with Peptide 5 (designated as Peptide 15). See text for amino acid sequence details. Choice of geometry relative to odorant molecules remains the same as in Peptide 1 and is shown in Figure 1 *g*.

takes place. The interaction energy is calculated by rotating the odorant molecule by 2π and simultaneously separating it from the peptide. The relative position of a given peptide is the same for all odorant molecules considered.

To investigate the effect of the increase in overall chirality of the peptide on the intermolecular interaction, we considered the addition of Peptides 2 and 5 (H–Pro–Met–Leu–Asn–Pro–OH sequence) to Peptide 1 and calculated the interaction profile with the corresponding dipeptide and odorants. Thus, keeping the relative position of carvone and Peptide 1, the interaction profile is investigated for H–Leu–His–Thr–Pro–Met–Met–Ala–Tyr–Asp–Arg–OH and H–Leu–His–Thr–Pro–Met–Leu–Asn–Pro–OH. These two higher peptides are designated as Peptides 12 and 15 respectively, and the structures are shown in Figure 2. The results are described in the next section.

Results and discussion

The calculated total interaction energy profiles (composed of nonbonded LJ potential and electrostatic Coulombic interaction potential) of Peptide 1 with enantiomeric carvones are shown in Figure 3 *a*, with a low value of dielectric constant ($\varepsilon_s = 4$) of the medium. In this case, *R*-carvone has more favourable interaction with Peptide 1 compared to *S*-carvone. This is consistent with the experimental fact that *R*-carvone is a stronger odorant compared to the *S*-carvone on threshold basis. The depths of the potential profiles for enantiomeric carvones are reduced with increase in dielectric constant ($\varepsilon_s = 20$), as shown in Figure 3 *b*. Thus the magnitude of favourable electrostatic interaction between the carvone and the peptide is reduced by increase in magnitude of the dielectric constant. However, chiral discrimination can still be observed in Figure 3 *b*. In contrast, the interaction profiles of Peptide 1 and enantiomers of camphor have no significant difference (Figure 3 *c*). As a result, the Peptide 1 cannot recognize the difference between enantiomers of camphor. The subtle difference observed between *RR*- and *SS*-enantiomers (Figure 3 *c*) is of the order of k_BT and thermal motion can destroy this small enantiodifference. The result is consistent with the fact that enantiomers of camphor do not have significant odour difference.

Differences in the orientation-dependent pair potential can be understood from the difference in chiral structure of carvone and camphor, as shown in Figure 4. Atoms (which act as interaction centres) of carvone are spatially less symmetrically distributed (Figure 4 *a*) and contained in two (approximately) asymmetrically oriented planes while atoms of the camphor molecule are distributed in three (approximately) more symmetrically distributed planes (Figure 4 *b*). The interaction centres of the camphor molecule are radially more distributed in space than carvone and the former has more periodic interaction (less orientation-dependent or more isotropic) with the given peptide compared to the latter. Thus, the peptide–carvone interaction profile shows more chiral discrimination than the peptide–camphor profile. This is consistent with our previous studies that ligand chirality plays a significant role in recognition by peptide[12]. As a point of caution, it may be noted that

both carvone and camphor are chiral and the planes in Figure 4 are drawn just to visualize the average planes on which a reasonable number of atoms of a given molecule can be placed, and have no relation with the plane of symmetry.

The capability of discrimination of carvone by Peptides 2 and 3 is less than that of Peptide 1 as shown in Figures 5 and 6. This is expected due to the fact that variation in chiral structure of the peptide leads to the difference in chiral recognition. In contrast, no enantiodifference is observed for camphor for Peptides 2 and 3. Plots for camphor are shown in Figures 5 *c* and 6 *c*, respectively. The interaction of Peptide 4 is more favourable with *S*-carvone than *R*-carvone, in contrast to the interaction with Peptides 1–3, as shown in Figure 7. This is consistent with the fact that one enantiomeric molecule may have less favourable interaction with a particular peptide, but may have favourable interaction with other peptides depending on the chiral structure of the peptide. Significantly, camphor is not discriminated by Peptide 4 like other peptides.

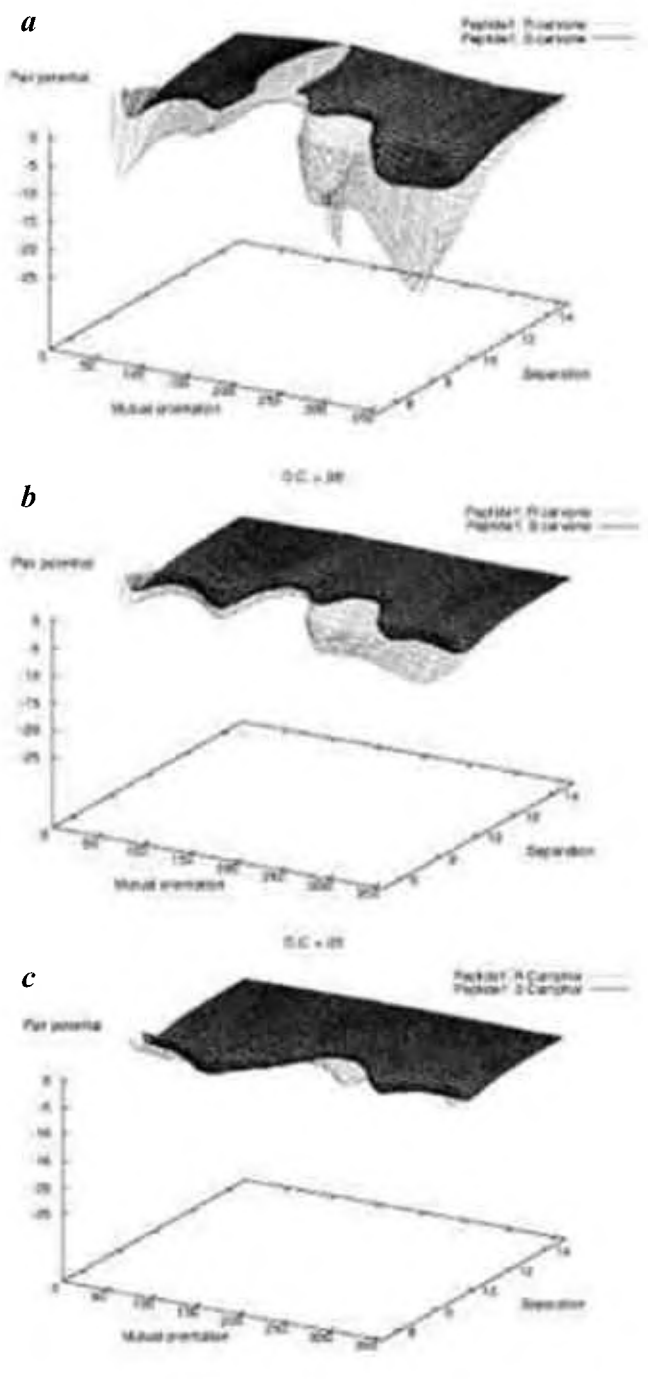

Figure 3. Interaction profile of Peptide 1 with (***a***) *R*- and *S*-carvone with $\varepsilon_s = 4$, ***b***, *R*- and *S*-carvone with $\varepsilon_s = 20$ and ***c***, *RR*- and *SS*-camphor with $\varepsilon_s = 20$. Plots with dotted lines correspond to *R*-enantiomer and those with solid lines correspond to *S*-enantiomer.

The peptide–carvone interaction profiles shown in Figures 3, 5–7 clearly show that the all peptide sequences can discriminate between the *R*- and *S*-enantiomers of carvone. This conclusion corroborates the recent coarse-grained calculation that the interaction profiles of chiral helical peptide with chiral ligand are different for two enantiomers of the ligand[18]. Thus, each peptide segment of a receptor transmembrane helix present in the membrane can have different orientation-dependent interaction with each enantiomer. This leads to the remarkable capacity of relatively less number of receptors to distinguish the enormous variety of odorant molecules.

However, Peptides 1–4 could only be considered as mimics of small fragments of the large transmembrane helix. Does the higher level organization (for example, larger secondary level helical structure or more organized tertiary level structure) have further influence on the interaction? Explicitly, it is worthwhile to investigate the effect of the surrounding chiral subunits over the interaction of chiral peptide units closest to the approaching ligand. Coarse-grained model showed that increasing chirality of the helical peptide (more spatially dissymmetric arrangement of amino acid residues) leads to increasing dissymmetry of the potential profile (becomes more orientation-specific)[12]. The potential profiles of the two higher peptides (namely Peptides 12 and 15) are expected to be more orientation-specific than the lower peptides, such as Peptide 1. The interaction profiles for Peptides 12 and 15 with enantiomeric carvone are shown in Figure 8 *a* and *b*, respectively. The plots show that the nature of the potential profile becomes more funnel-like in the former higher peptides. The funnel shape of the potential profile drives the interaction between the carvone and peptide as more orientation-specific compared to the case where the interaction profile has multiple minima (for example, with Peptides 1, 2 or 5). Thus, it is expected that the increasing diversity in peptide sequence in the helical structure will lead to better discrimination of enantiomeric odorants by the peptide. This explains the necessity of hypervariability of amino acid sequence in receptor proteins, which leads to higher-order chirality of variable degree.

In the present article, one representative mutual spatial arrangement between peptide and odorant is considered.

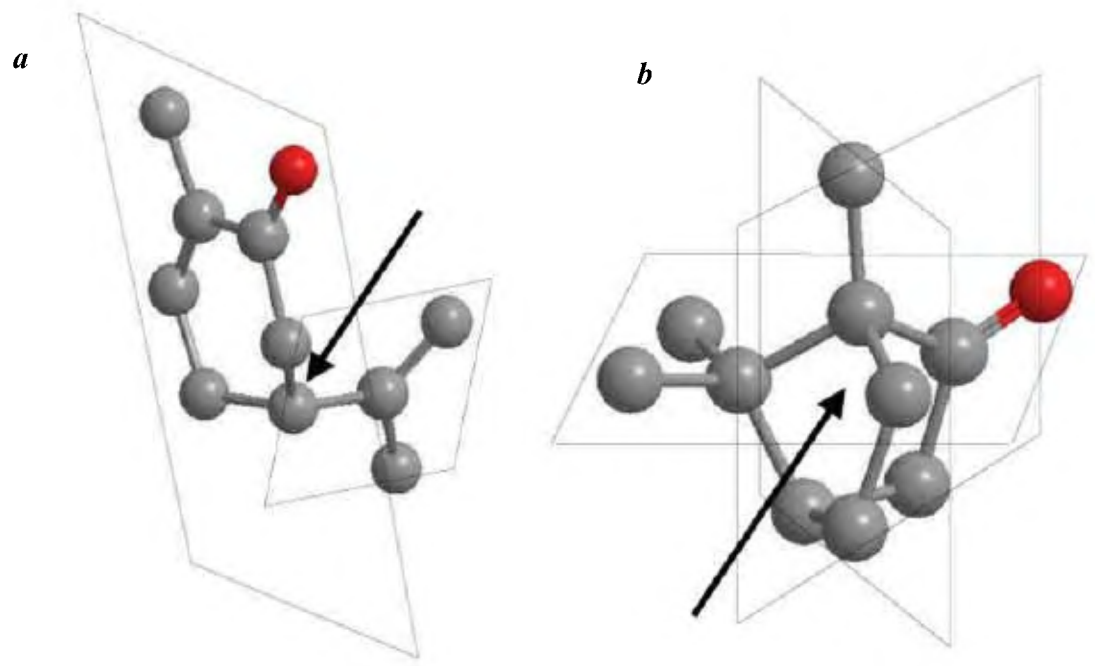

Figure 4. ***a***, Imaginary planes that contain a number of atoms of carvone and asymmetric orientation of these planes. ***b***, Similar planes containing a number of atoms of camphor are distributed in approximately three symmetrically distributed planes. The planes are an indication of the more globular structure of camphor compared to the planar structure of carvone and have no relation with the plane of symmetry. More spatially distributed interaction centres are present in camphor compared to carvone.

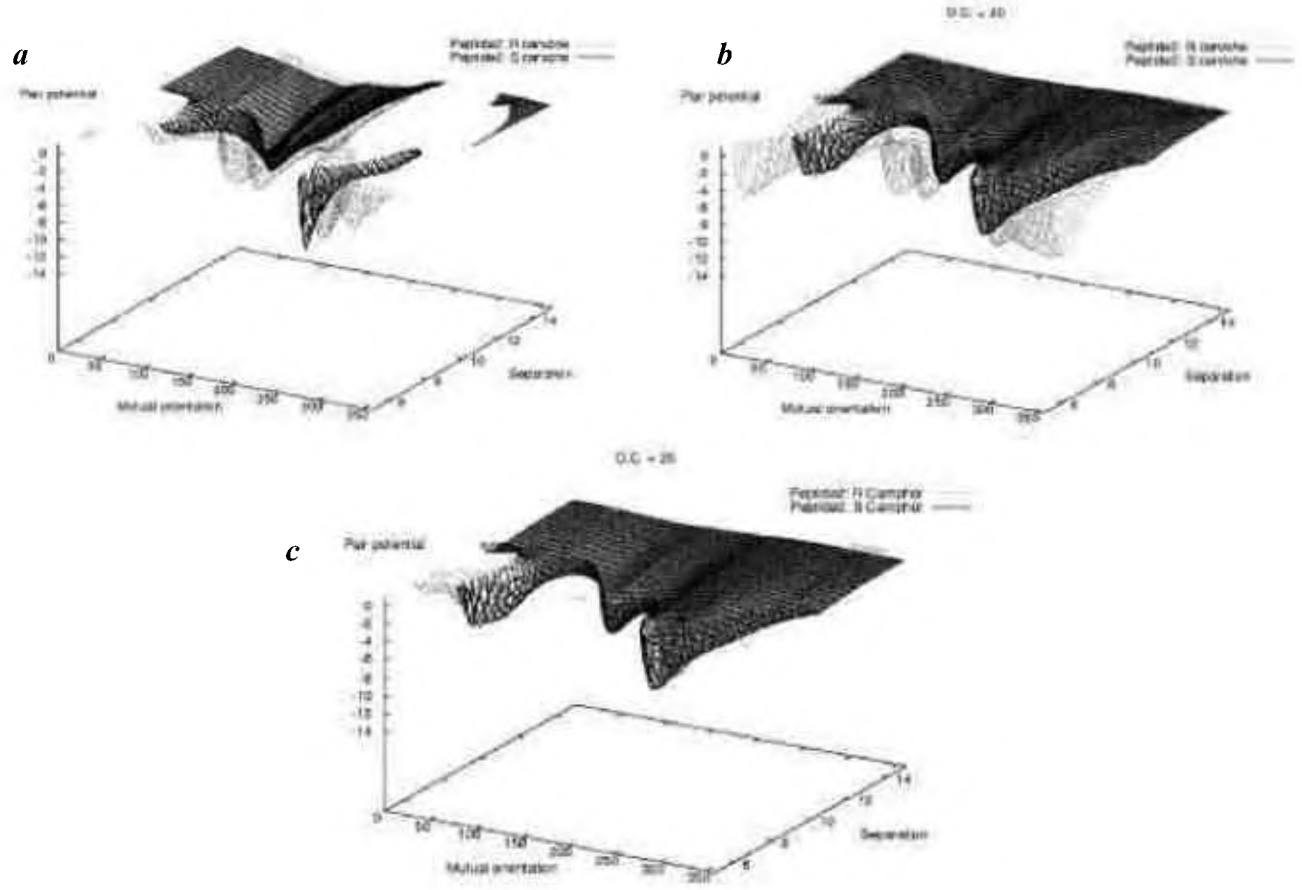

Figure 5. Interaction profile of Peptide 2 with (***a***) *R*- and *S*-carvone with $\varepsilon_s = 4$, (***b***) *R*- and *S*-carvone with $\varepsilon_s = 20$ and (***c***) *RR*- and *SS*-camphor with $\varepsilon_s = 20$. Plots with dotted lines correspond to *R*-enantiomer and those with solid lines correspond to *S*-enantiomer.

However, a number of mutual positions and orientations between peptide and odorant are possible[12], that may have varying degrees of stability of odorant binding. The global minima may be most effective in binding the odorant. Related conformational changes may control the signal transduction event and resulting odour characteristics. However, the other minima can also be effective in binding (according to Boltzmann distribution) depending on the availability of sufficient number of odorant molecules in proximity of the peptide at the corresponding mutual spatial separations and orientations. As a result, depending on the concentration of the odorant, the nature of binding with the peptide may vary. This is consistent with the fact that odour characteristic of odorants depends on concen-

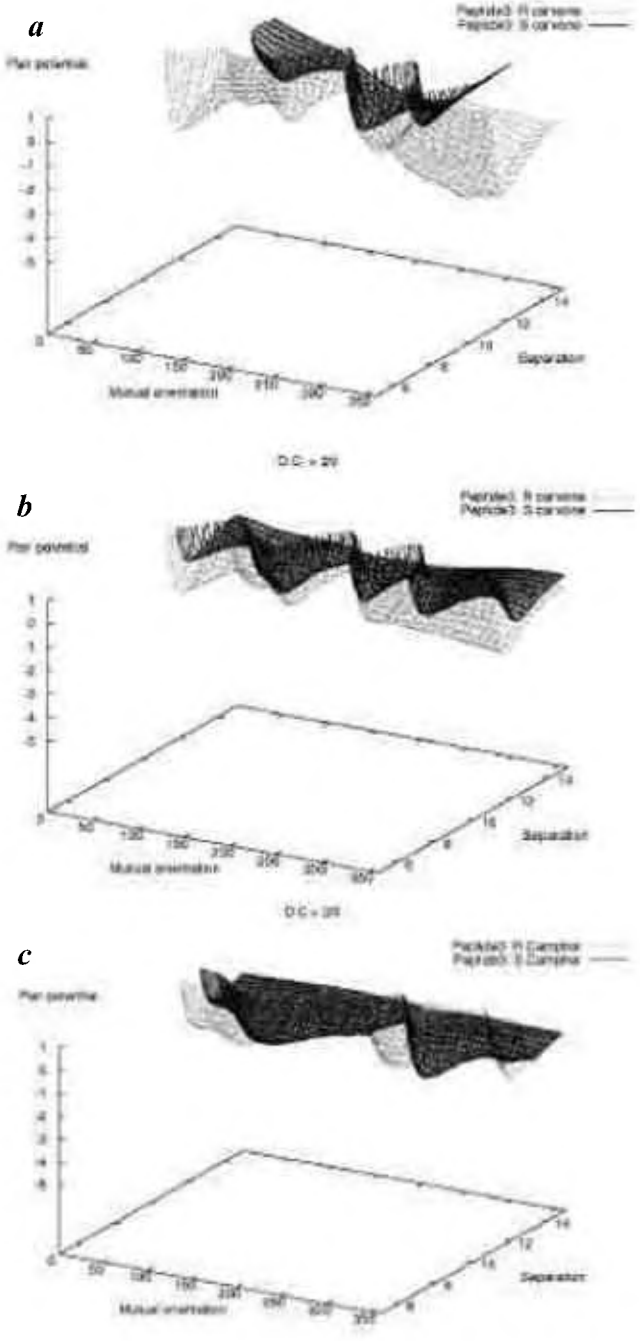

Figure 6. Interaction profile of Peptide 3 with (***a***) *R*- and *S*-carvone with $\varepsilon_s = 4$, (***b***) *R*- and *S*-carvone with $\varepsilon_s = 20$ and (***c***) *RR*- and *SS*-camphor with $\varepsilon_s = 20$. Plots with dotted lines correspond to *R*-enantiomer and those with solid lines correspond to *S*-enantiomer.

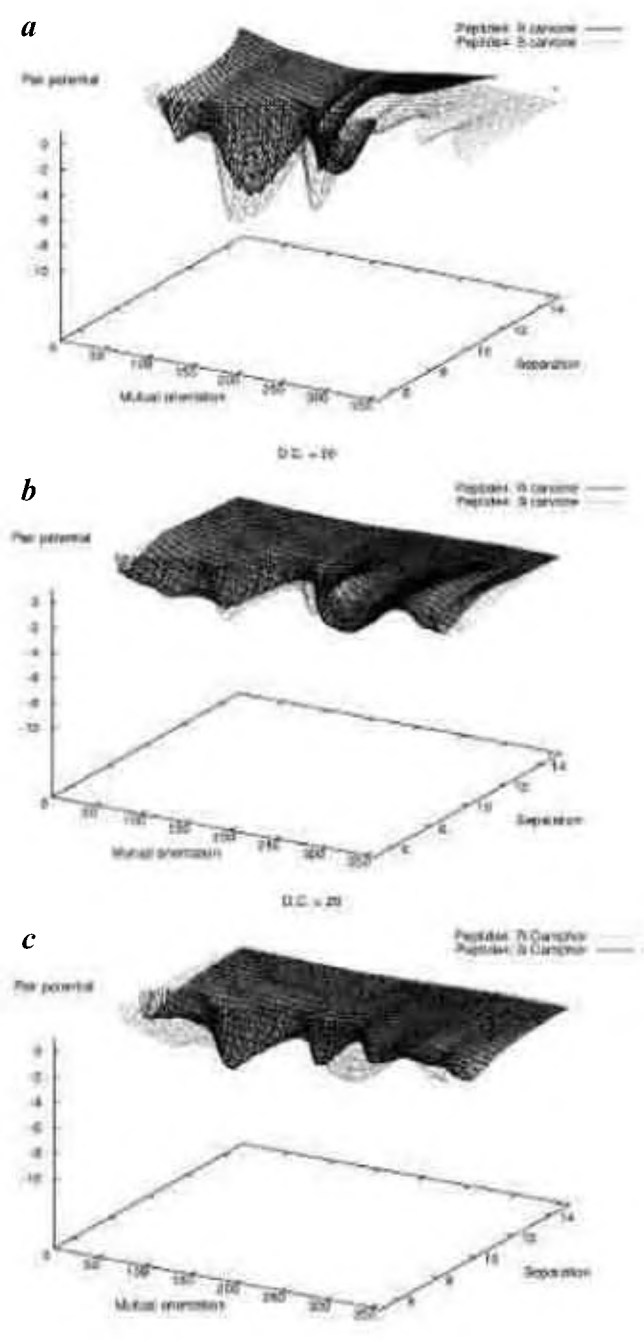

Figure 7. Interaction profile of Peptide 4 with (***a***) *R*- and *S*-carvone with $\varepsilon_s = 4$, (***b***) *R*- and *S*-carvone with $\varepsilon_s = 20$ and (***c***) *RR*- and *SS*-camphor with $\varepsilon_s = 20$. Plots with solid lines correspond to *R*-enantiomer and those with dotted lines correspond to *S*-enantiomer.

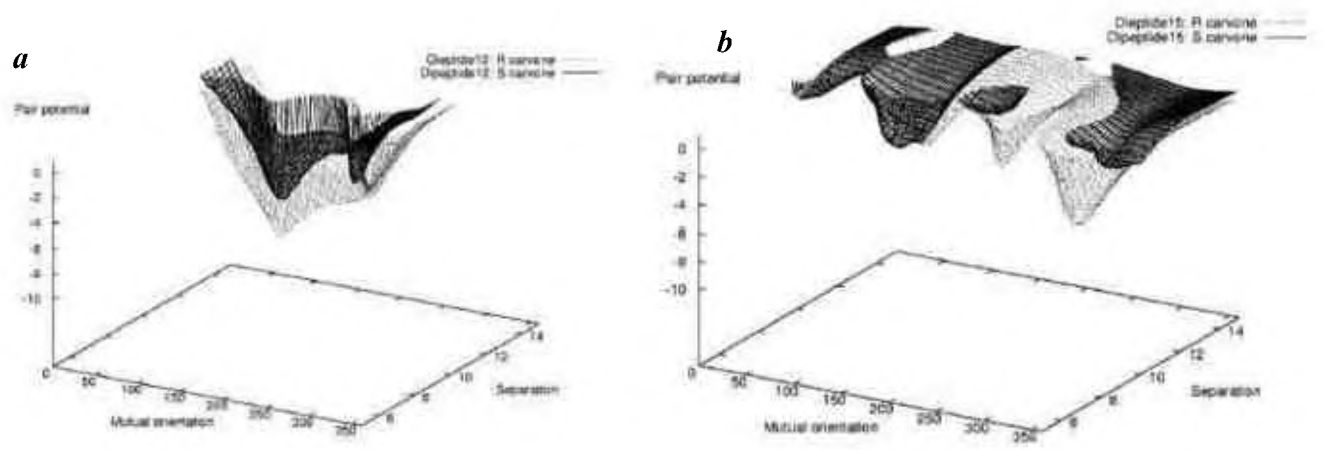

Figure 8. Interaction profile of (***a***) dipeptide 12 and (***b***) dipeptide 15 with *R*- and *S*-carvone with $\varepsilon_s = 4$.

tration. The intensity of the signal is expected to be dependent on the total interaction energy. As a result, a threshold concentration of odorants is always required, which is dependent on the shape and depth of the corresponding potential well. This is consistent with the well-known fact that different odorants have varying degrees of threshold concentration.

Buck and Axel[19] have pointed out that individual subfamilies of genes may encode receptors that bind distinct structural classes of odorant. The degree of variability of the residue is less among the subfamily and may recognize more subtle variation among odour molecules of a given class. Such a model indicates that activation of distinct receptors with similar structure could give rise to different odours, because the perceived odour will depend on higher-order processing and this model is in contrast with the stereochemical theory. The present calculation indicates that the discrimination could start even at the level of initial recognition by OR. One chiral receptor will give rise to different molecular interactions with odorant molecules that may belong to the same class of structure, but have subtle stereochemical or conformational differences. As a result, the binding event and subsequent signal transduction are expected to be different for these odorants.

The present calculation also shows that the increase in chirality of the receptor fragment (as shown by dipeptide – odorant interaction) increases the specificity of binding with the ligand. Thus, at a given relative position and orientation, the recognition is more specific for enhanced chirality of the ligand. This draws our attention to the omnipresence of chirality in biological receptors. The enantiodifference of odorant molecules (or its absence) indicates that the chirality of molecular structure has a decisive role in molecular recognition events in biological systems. More systematic molecular studies using different classes of odorant with subtle variation in molecular structure are necessary and future studies are to be aimed in this direction.

Conclusion

The present calculation shows that the two enantiomers of an odorant could have different orientation-dependent favourable potential profile with different peptide molecules depending on the chiral molecular structure of the odorant. Details of the potential profile depend on the chirality of the odorant as well as the peptide. It is shown that despite the presence of chirality in both carvone and camphor molecules, the former enantiomeric pair can be discriminated, while the latter pair does not show significant enantiodifference. More spatial dissymmetry of carvone leads to successful enantiodifference in its odour perception compared to camphor. Two enantiomers of carvone molecule have favourable interaction with different peptides with varying degree of stability and mutual orientation. This result is consistent with the fact that the identified receptor subtypes respond not to one but to many odorants. The present calculation corroborates the fact that the naturally occurring hypervariability of amino acid sequence is used to recognize the wide variety of odorants. Variation in sequence leads to diverse chiral structures, each of which can successfully recognize multiple odorants. According to the present calculation, a threshold concentration of odorants is always required to bind with the receptor that is dependent on the shape and depth of the corresponding potential well. This is consistent with the well-known fact that different odorants have varying degrees of threshold concentration. In the present work it is shown that olfactory discrimination could start even at the level of initial recognition by OR. A given chiral receptor will have different molecular interactions with a number of odorant molecules that may belong to the same class of structure, but have subtle stereochemical or conformational differences. As a result, the binding event and subsequent signal transduction are expected to be different for these odorants. The present calculation also corroborates the fact

that the multiple odorant receptors can recognize a particular odorant and different odorants are recognized by distinct combinations of the receptors.

1. Nandi, N. and Vollhardt, D., *Chem. Rev.*, 2003, **103**, 4033–4075.
2. Nandi, N. and Vollhardt, D., *Thin Solid Films*, 2003, **433**, 12–21.
3. Pathirana, S., Neely, W. C., Myers, L. J. and Vodyanoy, V., *J. Am. Chem. Soc.*, 1992, **114**, 1404–1405; Pathirana, S., Neely, W. C. and Vodyanoy, V., *Langmuir*, 1998, **14**, 679–682.
4. Leitereg, T. J., Gudagni, D. G., Harris, J., Mon, T. R. and Teranishi, R., *Nature*, 1971, **230**, 455–456.
5. Nandi, N., *J. Phys. Chem. A*, 2003, **107**, 4588–4591.
6. Laska, M. and Teubner, P., *Chem. Senses*, 1999, **24**, 161–170; Laska, M., *Chem. Senses*, 2004, **29**, 143–152.
7. Kraft, P. and Fráter, G., *Chirality*, 2001, **13**, 388–394; Fráter, G., Müller, U. and Kraft, P., *Helv. Chem. Acta*, 1999, **82**, 1656–1665.
8. www.leffingwell.com; © Leffingwell and Associates.
9. Amoore, J. E., *Nature*, 1963, **198**, 271–272; Amoore, J. E., In *Molecular Basis of Odor*, Charles C. Thomas, Springfield III, 1970.
10. Wright, R. H. and Robson, A., *Nature*, 1969, **222**, 290–292; Wright, R. H. and Burgess, R. E., In *Gustation and Olfaction* (eds Ohloff, G. and Thomas, A. F.), Academic Press, 1971, pp. 134–144.
11. Turin, L., *J. Theor. Biol.*, 2002, **216**, 367–385.
12. Nandi, N., *J. Phys. Chem. B*, 2004, **108**, 789–797.
13. Hansen, J. P. and McDonald, I. R., *Theory of Simple Liquids*, Academic Press, London, 1976.
14. Reviews in the special issue on olfaction, *Science*, 1999, **286**, 703–728.
15. CS MOPAC® Pro component of CHEM 3D Ultra software; © Cambridge Soft Corporation, 1985–2003.
16. Stewart, J. J. P., *J. Comput. Chem.*, 1989, **10**, 209–220.
17. Jensen, F., *Introduction to Computational Chemistry*, 1999, pp. 81–99.
18. Jorgensen, W. and Tirado-Rives, J., *J. Am. Chem. Soc.*, 1988, **110**, 1657–1666.
19. Buck, L. and Axel, R., *Cell*, 1991, **66**, 175–187.

ACKNOWLEDGEMENTS. The present work is supported by a grant to the author from CSIR, New Delhi. Thanks are due to Mr K. Thirumoorthy for a critical reading of the manuscript.

Received 26 November 2004; revised accepted 11 March 2005